

Subpixel smoothing for conductive and dispersive media in the finite-difference time-domain method

Alexei Deinega^{1,*} and Ilya Valuev²

¹*Kinetic Technologies Ltd., 1 Kurchatov Square, Moscow 123182, Russia*

²*Joint Institute for High Temperatures of RAS, 13/19 Izhorskaya Street, Moscow 125412, Russia*

*Corresponding author: poblizosti@kintech.ru

Received July 23, 2007; accepted September 25, 2007;
posted November 2, 2007 (Doc. ID 85600); published November 27, 2007

Staircasing of media properties is one of the intrinsic problems of the finite-difference time-domain method, which reduces its accuracy. There are different approaches for solving this problem, and the most successful of them are based on correct approximation of inverse permittivity tensor $\hat{\epsilon}^{-1}$ at the material interface. We report an application of this tensor method for conductive and dispersive media. For validation, comparisons with analytical solutions and various other subpixel smoothing methods are performed for the Mie scattering from a small sphere. © 2007 Optical Society of America

OCIS codes: 000.4430.

The finite-difference time-domain (FDTD) method [1] is an extensively used computational tool in electrodynamics. There are several reasons for its popularity: explicit time stepping does not involve slow matrix operations, the method provides a solution in the natural form of time-dependent fields, and it is suitable for nonlinear media and complex geometry simulation. However, as for any other finite-difference method, there exists an intrinsic problem of discretization of media properties on the FDTD space grid. In the vicinity of discontinuity of material properties the Maxwell equations should be solved, taking interface boundary conditions for electric and magnetic fields into account. Any curved media interface that cannot be aligned with the FDTD grid is distorted by staircasing, which reduces the accuracy of calculation. Thus a particular local interface orientation becomes important.

Various models were proposed for solving this problem within FDTD. There is a class of methods that are based on the modification of the discretization mesh to better match the interface. For example, finer grids [2] may be introduced in the regions with complex geometry. Another possible way of reducing the staircase effect is irregular nonorthogonal mesh generation according to the geometry of the objects [3]. Modification of the update scheme for selected mesh cells near the interface can also be introduced (contour path algorithm) [4]. Methods of this type either imply modification of the field update algorithms or introduce irregular meshes, which may significantly slow down performance.

Another class of methods is based on adjusting effective permittivity ϵ in the vicinity of an interface. Consider a volume $\delta x \times \delta y \times \delta z$ surrounding a chosen grid point and assume that it is crossed by an interface of two media with permittivities ϵ_1 and ϵ_2 . The interface boundary conditions for discretized \vec{E} and \vec{D} fields may be modeled by an inverse dielectric permittivity tensor of the following form [5–8]:

$$\hat{\epsilon}^{-1} = \mathbf{P}\langle\epsilon^{-1}\rangle + (\mathbf{1} - \mathbf{P})\langle\epsilon\rangle^{-1}, \quad (1)$$

where \mathbf{P} is the projection matrix $P_{ij} = n_i n_j$ onto the normal \vec{n} to the interface between two media and $\langle \rangle$ is the averaging over the volume. This expression was derived in [5] for the 2D case and then used with the omitted nondiagonal part of \mathbf{P} . The effective permittivity methods may be regarded as based on different approximations to (1). While the most straightforward way of smoothing permittivity is taking contour-average or volume-average $\langle\epsilon\rangle$ as an effective value for the field update cell [9], more sophisticated methods, such as the Kaneda formula [10] or the VP-EP formula [5], take the local direction \vec{n} of the interface into account. Partial implementation of the expression (1) results in numerical error scaled linearly with resolution. Full tensor \mathbf{P} implementation was performed in [6–8]. It was demonstrated that the full tensor method has quadratic accuracy with respect to space resolution [8]. So far the effective permittivity method has concerned only pure dielectrics. We develop a scheme [6–8] for conductive and dispersive media.

Consider an interface between two arbitrary conductive dispersive media with frequency-dependent complex permittivities $\epsilon_{1,2}(\omega)$. Expressing Ampere's law in the frequency domain using the effective permittivity tensor (1), we obtain

$$-i\omega\vec{E} = \mathbf{P} \left[\frac{f_1}{\epsilon_1(\omega)} + \frac{1-f_1}{\epsilon_2(\omega)} \right] (\nabla \times \vec{H}) + \frac{\mathbf{1} - \mathbf{P}}{f_1\epsilon_1(\omega) + (1-f_1)\epsilon_2(\omega)} (\nabla \times \vec{H}), \quad (2)$$

where f_1 is the fraction of the cell volume embedded in the first medium. To solve Eq. (2) in the time domain we represent \vec{E} as a sum of auxiliary variables according to the denominators of the terms in Eq. (2):

$$\vec{E} = \vec{E}^1 + \vec{E}^2 + \vec{E}^3, \quad (3)$$

$$-i\omega\epsilon_1(\omega)\vec{E}_k^1 = f_1 \sum_{j=1}^3 P_{kj}(\nabla \times \vec{H})_j, \quad (4)$$

$$-i\omega\epsilon_2(\omega)\vec{E}_k^2 = (1-f_1) \sum_{j=1}^3 P_{kj}(\nabla \times \vec{H})_j, \quad (5)$$

$$\begin{aligned} -i\omega[f_1\epsilon_1(\omega) + (1-f_1)\epsilon_2(\omega)]\vec{E}_k^3 \\ = (\nabla \times \vec{H})_k - \sum_{j=1}^3 P_{kj}(\nabla \times \vec{H})_j. \end{aligned} \quad (6)$$

The equations for \vec{E}^m can be solved in the time domain in the usual way. For example, if permittivities $\epsilon_1(\omega)$, $\epsilon_2(\omega)$ consist of arbitrary number of Debye, Drude, and Lorentz terms, one can use the auxiliary differential equation method [11]. We implemented the solution of Eqs. (3)–(6) as part of the generic contour-based EMTL simulation library [12]. Evaluation of the interface normal vector and medium fraction f_1 is performed on the setup phase by analyzing media inside a 3D body drawn around an update contour center. This averaging body is usually a box equal in volume to the Yee cell. The auxiliary vectors \vec{E}^m are always normal to the update contour plane, thus only one scalar projection of \vec{E}^m is needed for each contour. The diagonal terms of $P_{kj}(\nabla \times \vec{H})_j$, $j=k$ are evaluated within the standard fast bulk contour update procedure, while the nondiagonal terms $j \neq k$ are obtained from linear space interpolation of \vec{H} , generically provided by EMTL. The addition of nondiagonal terms, time stepping, and summation of \vec{E}^m are performed at the end of the bulk time step, composing a special smoothing “fix” within EMTL.

To verify the accuracy of our method we compare it with Mie scattering theory [13]. The explicit time stepping is performed using a uniform Yee mesh. We use the total field/scattered field method [1] with Berenger impulse $(t-t_0)\exp(-(t-t_0)^2/t_{decay}^2)$ for generation of a test plane wave impinging a spherical body of small size of the order of the mesh space step. The sphere is centered within one of the Yee mesh cells.

The calculated space (Fig. 1) is surrounded by absorbing walls implemented as uniaxial perfectly matched layers [1]. The fields near the sphere are measured by near detectors, forming a closed surface. Near-to-far-field transformation [1] is used to obtain the fields at virtual far detectors at a distance of about 1000 simulation box widths from the sphere.

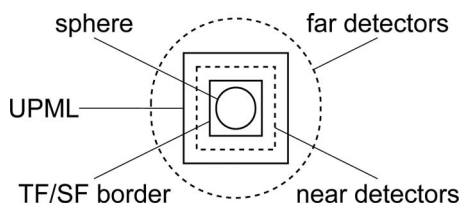


Fig. 1. Schematic view of the simulation geometry.

The fields at the far detectors are used for comparing scattering properties with the Mie theory.

The following effective permittivity methods were compared in our Mie scattering tests: (a) staircase with permittivity properties taken at the field update contour center, (b) averaging of the dispersive permittivity terms over either the update contour surface or the Yee cell volume, (c) harmonic averaging corresponding to setting $\mathbf{P}=\mathbf{1}$ in Eq. (2), (d) the VP-EP method [5] modified for conductive and dispersive media and corresponding to the diagonal part of Eq. (1), and (e) the full tensor method. For most numerical tests the efficiency factor for scattering, being the scattering cross section normalized by the effective object size $Q_{sca} = S/(4\pi r^2)$, is used as an output.

In the first test series we consider scattering from a conductive sphere for various sphere radii (Fig. 2). The jumps in the measured scattering cross section for staircase and contour averaging methods result from a discontinuous change in field update coefficients as new Yee contours cross the sphere while increasing the radius. For volume averaging the curves are much smoother. One can conclude that averaging over control volume rather than over a surface is important for distinguishing very small objects but does not improve accuracy for other scales. Note that the direct and harmonic average curves lie at the opposite sides of the theoretical curve. The tensor methods implement the proper mix of both kinds of averaging (the results for tensor methods are indistinguishable from the theoretical curve in Fig. 2). A comparison of the accuracy for different methods is given in Fig. 3 as a function of mesh resolution.

In the second test series we consider scattering from a lead sphere for $\lambda = 1.5 \mu\text{m}$ simulated by a mesh with space step $\Delta r = 50 \text{ nm}$ (Figs. 4 and 5). We use Drude approximation $\epsilon(\omega) = \epsilon_\infty - [\omega_{pl}^2/(\omega^2 + i\omega\gamma)]$ for dispersive permittivity of lead with particular parameter values taken from [14]. All methods, especially based on simple averaging, demonstrate lower accuracy than in the previous conductive sphere case. For the wavelength considered the permittivity of lead is $\epsilon \approx -81 + 18i$, thus the real part of ϵ is negative. Since the solution of the Maxwell equations is essentially different in regions of positive and nega-

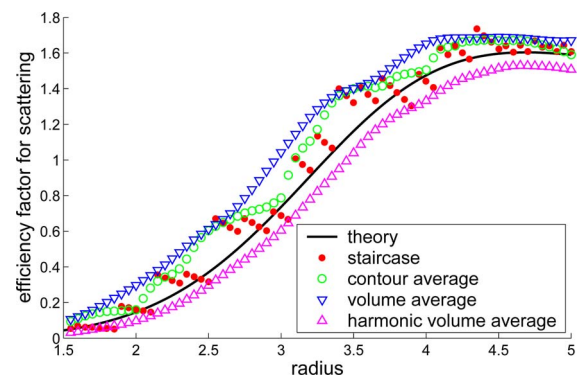


Fig. 2. (Color online) Efficiency factor for scattering Q_{sca} versus radius for a conductive sphere with $\epsilon = 4\epsilon_0$ and $\sigma = 2$ at $\lambda = 25$. The length is measured in the mesh space steps.

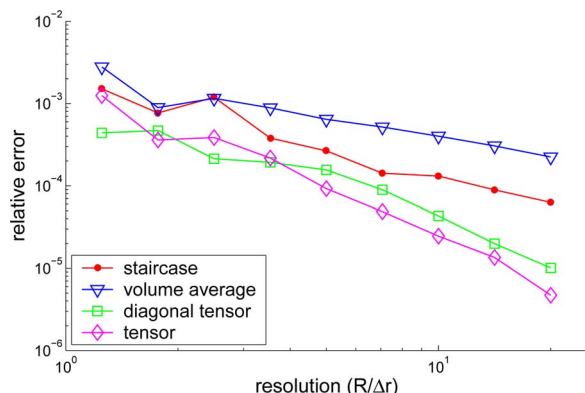


Fig. 3. (Color online) Error relative to the Mie theory for Q_{sca} and the setup of the Fig. 2 as a function of the sphere radius R .

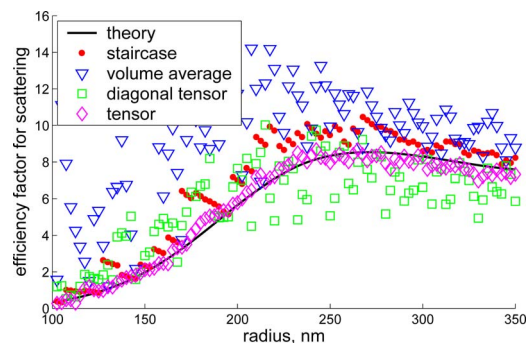


Fig. 4. (Color online) Efficiency factor for scattering Q_{sca} versus radius for lead sphere, $\lambda = 1.5 \mu\text{m}$.

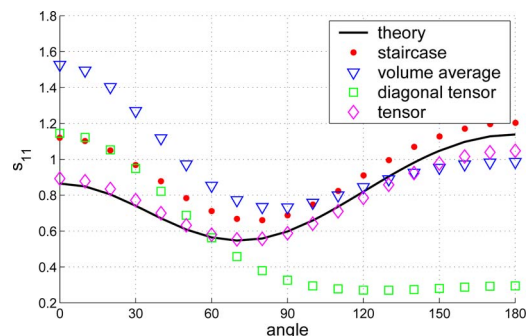


Fig. 5. (Color online) S_{11} scattering matrix element of lead $r = 250 \text{ nm}$ sphere as a function of the scattering angle, $\lambda = 1.5 \mu\text{m}$.

tive ϵ , the methods that do not take the interface direction into account, including the diagonal tensor method, fail to improve accuracy compared with the staircase model. For angular dependence of the scattering matrix element S_{11} [13] the full tensor method has the best accuracy in the whole scattering angle range (Fig. 5).

In the present work we demonstrated the successful implementation of a tensor subpixel smoothing method for conductive and dispersive media. It was shown that keeping off-diagonal elements of the effective inverse permittivity tensor is crucial for correct representation of the scattering properties of small objects.

This work is partially supported by research program 15 of the Russian Academy of Science.

References

1. A. Taflove and S. H. Hagness, *Computational Electrodynamics: the Finite Difference Time-Domain Method* (Artech House, 2000).
2. S. S. Zivanovic, K. S. Yee, and K. K. Mei, *IEEE Trans. Microwave Theory Tech.* **38**, 471 (1991).
3. V. Shankar, A. Mohammadian, and W. F. Hall, *Electromagnetics* **10**, 127 (1990).
4. T. G. Jurgens, A. Taflove, K. Umashankar, and T. G. Moore, *IEEE Trans. Antennas Propag.* **40**, 357 (1992).
5. A. Mohammadi, H. Nadgaran, and M. Agio, *Opt. Express* **13**, 10367 (2005).
6. J.-Y. Lee and N.-H. Myung, *Microwave Opt. Technol. Lett.* **23**, 245 (1999).
7. J. Nadobny, D. Sullivan, W. Wlodarczyk, P. Deuffhard, and P. Wust, *Lect. Notes Math.* **51**, 1760 (2003).
8. A. Farjadpour, D. Roundy, A. Rodriguez, M. Ibanescu, P. Bermel, J. D. Joannopoulos, S. G. Johnson, and G. Burr, *Opt. Lett.* **31**, 2972 (2006).
9. S. Dey and R. Mittra, *IEEE Trans. Microwave Theory Tech.* **47**, 1737 (1999).
10. N. Kaneda, B. Houshmand, and T. Itoh, *IEEE Trans. Microwave Theory Tech.* **45**, 1645 (1997).
11. M. Okoniewski, M. Mrozowski, and M. A. Stuchly, *IEEE Microw. Guid. Wave Lett.* **7**, 123 (1997).
12. I. Valuev, A. Deinega, A. Knizhnik, and B. Potapkin, *Lect. Notes Comput. Sci.* **4707**, 213 (2007).
13. C. F. Bohren and D. R. Huffman, *Absorption and Scattering of Light by Small Particles* (Wiley-Interscience, 1983).
14. M. A. Ordal, L. L. Long, R. J. Bell, S. E. Bell, R. R. Bell, R. W. Alexander, Jr., and C. A. Ward, *Appl. Opt.* **22**, 1099 (1983).